Carbohydrate Polymers 82 (2010) 670–679

Contents lists available at ScienceDirect

Carbohydrate Polymers

journal homepage: www.elsevier.com/locate/carbpol

Gum kondagogu (*Cochlospermum gossypium*): A template for the green synthesis and stabilization of silver nanoparticles with antibacterial application

Aruna Jyothi Kora [a], R.B. Sashidhar [b,*], J. Arunachalam [a]

[a] National Centre for Compositional Characterisation of Materials (NCCCM), Bhabha Atomic Research Centre, ECIL PO, Hyderabad 500 062, India
[b] Department of Biochemistry, University College of Science, Osmania University, Hyderabad 500 007, Andhra Pradesh, India

ARTICLE INFO

Article history:
Received 22 February 2010
Received in revised form 5 May 2010
Accepted 18 May 2010
Available online 25 May 2010

Keywords:
Autoclaving
Natural gum
Silver nanoparticles
Surface-enhanced Raman scattering (SERS)
Antibacterial

ABSTRACT

A facile and ecofriendly method has been developed for the synthesis of silver nanoparticles from silver nitrate using gum kondagogu (*Cochlospermum gossypium*) a natural biopolymer, as a reducing and stabilizing agent. The influence of different parameters such as gum particle size, concentration of gum, concentration of silver nitrate and reaction time on the synthesis of nanoparticles was studied. The synthesized nanoparticles were characterized using UV–visible spectroscopy, transmission electron microscopy, X-ray diffraction and thermogravimetric analysis. By optimizing the reaction conditions, we could achieve nearly monodispersed and size controlled spherical nanoparticles of around 3 nm. A possible mechanism involved in the reduction and stabilization of nanoparticles has been investigated using Fourier transform infrared spectroscopy and Raman spectroscopy. The synthesized silver nanoparticles had significant antibacterial action on both the Gram classes of bacteria. As the silver nanoparticles are encapsulated with functional group rich gum, they can be easily integrated for various applications.

1. Introduction

Silver nanoparticles are of considerable interest owing to their distinctive electrical, electronic, thermal, optical, magnetic, catalytic, sensing and antimicrobial functionalities compared to bulk metal (Cho, Park, Osaka, & Park, 2005; Reddy, Lee, Lee, & Gopalan, 2008; Wei & Qian, 2008); those are related to physical properties such as size, shape and inter-particle spacing (Jonathan, Amanda, Adam, Chanda, & Richard, 2003). Of which, the antimicrobial properties of silver nanoparticles have several biotechnological applications including: nanosilver coated or impregnated ceramic water filters, activated carbon air filters, catheters (Sharma, Yngard, & Lin, 2009), wound dressings (Maneerung, Tokura, & Rujiravanit, 2008; Totaro & Rambaldini, 2009), and biodegradable poly(L-lactide) (PLA) fibres (Xu et al., 2006). The antimicrobial activity of silver and its compounds is well established and it has wide antibacterial spectrum (Mahapatra & Karak, 2008; Tiwari, Behari, & Sen, 2008; Xu, Wang, Kang, & Chen, 2009; Yang, Wu, Liu, Lin, & Hu, 2009). In addition, silver is known to exhibit oligodynamic effect because of its ability to exert bactericidal activity at minute concentrations (Tien, Tseng, Liao, & Tsung, 2009). The development of resistance to silver in microbes is improbable due to its action on a broad spectrum of targets in the cell (Inoue et al., 2002). The advantage of silver nanoparticles compared to bulk metal or salts is the slow and regulated release of silver from nanoparticles thereby causing long lasting protection against bacteria (Totaro & Rambaldini, 2009).

A survey of earlier literature suggests that various synthetic and natural polymers such as poly(ethylene glycol) (PEG) (Luo, Zhang, Zeng, Zeng, & Wang, 2005), poly-(N-vinyl-2-pyrrolidone) (PVP) (Xiong et al., 2006), starch (Vigneshwaran, Nachane, Balasubramanya, & Varadarajan, 2006) heparin, and chitosan (Huang & Yang, 2004) have been reported as reducing agents for the synthesis of silver and gold nanoparticles. Sodium alginate a polysaccharide gum derived from the cell walls of brown algae, has been used as a reducing and stabilizing agent for the synthesis of gold nanoparticles (Pal, Esumi, & Pal, 2005). It has been demonstrated that the plant based exudate gum such as gum Acacia can be utilized as a reducing and stabilizing agent for the silver nanoparticle biosynthesis (Mohan, Raju, Sambasivudu, Singh, & Sreedhar, 2007). Recently gum gellan, a microbial heteropolysaccharide secreted from *Sphingomonas elodea* was employed for similar purpose in the case of gold nanoparticles (Dhar, Reddy, Shiras, Pokharkar, & Prasad, 2008). Gum kondagogu is a naturally occurring non-toxic polysaccharide derived as an exudate from the bark of *Cochlospermum gossypium* (Bixaceae family), a native tree of India. This native Indian gum is collected by the tribals from the forests of Andhra Pradesh state, which is one of the major gum producing centers in India and marketed through Girijan Co-operative Corporation Ltd., Visakhapatnam, India. As the gum

* Corresponding author. Tel.: +91 40 27097044; fax: +91 40 27097044.
E-mail address: sashi_rao@yahoo.com (R.B. Sashidhar).

0144-8617/$ – see front matter © 2010 Elsevier Ltd. All rights reserved.
doi:10.1016/j.carbpol.2010.05.034

kondagogu does not have an independent identity in the world market, it was earlier grouped under gum karaya and exported along with gum karaya (Janaki & Sashidhar, 1998, 2000). To exploit its potential commercial applications, its morphological, structural, physicochemical, compositional, solution, conformational, rheological, emulsifying and metal-biosorption properties have been well characterized and studied (Janaki & Sashidhar, 1998; Vegi et al., 2009; Vinod & Sashidhar, 2009; Vinod, Sashidhar, Sarma, & Saradhi, 2008; Vinod, Sashidhar, Sreedhar, et al., 2009; Vinod, Sashidhar, & Sukumar, 2009; Vinod, Sashidhar, Suresh, et al., 2008). The primary structure this gum is made up of sugars such as arabinose, galactose, glucose, mannose, rhamnose, glucuronic acid and galacturonic acid with sugar linkage of (1 → 2) β-D-Gal p, (1 → 6) β-D-Gal p, (1 → 4) β-D-Glc p A, 4-O-Me-α-D-Glc p A, (1 → 2) α-L-Rha and has a molecular weight of 7.2×10^6 Da (Vinod & Sashidhar, 2009; Vinod, Sashidhar, Sarma, et al., 2008; Vinod, Sashidhar, Suresh, et al., 2008). Earlier studies have established that gum kondagogu is non-toxic and has a potential application as a food additive and as a drug delivery matrix (Janaki & Sashidhar, 2000; Naidu et al., 2009). The interesting features of gum kondagogu motivated us to use this biopolymer as a template for the synthesis and stabilization of silver nanoparticles due to (i) its natural availability and low cost; (ii) it is also non-toxic and a potential food additive; (iii) abundant in hydroxyl, acetyl, carbonyl and carboxylic functional groups and (iv) its metal-biosorption properties.

The green synthesis of inherently safer silver nanoparticles depends on the adoption of the basic requirements of green chemistry; the solvent medium, the benign reducing agent and the non-hazardous stabilizing agent (Vigneshwaran et al., 2006). In this context, we have explored and developed a facile and green route for the synthesis of silver nanoparticles using a non-toxic, renewable natural plant polymer, gum kondagogu as both the reducing and stabilizing agent. Being a natural polymer, gum kondagogu is amenable for biodegradation. The synthesis was carried out in aqueous medium without the requirement of any added chemical reducing agent by autoclaving. In this study, autoclaving was adopted as a synthetic route to produce sterile silver nanoparticles that are completely free from bacteria, viruses and spores, which may find biological applications. The focus of the present study was on (i) the synthesis, (ii) characterization and (iii) capping and stabilization of silver nanoparticles. In addition, we have also demonstrated the antibacterial activity of the prepared nanoparticles on Gram-positive and Gram-negative bacteria for finding out the potential of the generated nanoparticles for various environmental and biomedical applications.

2. Experimental

2.1. Synthesis of silver nanoparticles

Silver nitrate ($AgNO_3$) ((E. Merck, Mumbai, India) of analytical reagent grade was used for the synthesis. "Gum kondagogu", grade 1 was purchased from Girijan Cooperative Corporation, Hyderabad, India. All the solutions were prepared in ultra pure water. Gum kondagogu was powdered in a high-speed mechanical blender (Prestige, Bangalore, India) and sieved to obtain a mean particle size of 300, 105 and 38 μm. Then 0.5% (w/v) of homogenous gum stock solution was prepared by adding this powder to reagent bottle containing ultra pure water and stirring overnight at room temperature. The silver nanoparticles were synthesized by autoclaving the silver nitrate solutions containing various concentrations of gum kondagogu (KG) at 121 °C and 15 psi for different durations of time. The effect of different parameters such as (i) gum particle size, (ii) concentration of gum, (iii) concentration of silver nitrate and (iv) reaction time on nanoparticle synthesis was studied.

2.2. Characterization of synthesized silver nanoparticles

In order to study the formation of silver nanoparticles, the UV–visible absorption spectra of the prepared colloidal solutions were recorded using an Elico SL 196 spectrophotometer (Hyderabad, India), from 250 to 800 nm, against autoclaved gum blank. The absorption spectra of gum before and after autoclaving were also recorded against ultra pure water blank. The size and shape of the nanoparticles were obtained with Hitachi H 7500 (Tokyo, Japan) and JEOL 3010 (Tokyo, Japan) transmission electron microscopes (TEM), operating at 80 kV and 200 kV, respectively. Samples were prepared by depositing a drop of colloidal solution on a carbon coated copper grid and drying at room temperature. The solutions of the synthesized nanoparticles were lyophilized and recovered in powdered form using a Heto-Holten A/S, DK-3450 freeze dryer (Allerd, Denmark). The X-ray diffraction analysis was conducted with a STOE powder diffractometer (Darmstadt, Germany) using monochromatic Cu Kα radiation (λ = 1.5406 Å) running at 40 kV and 30 mA. The intensity data for the lyophilized nanosilver powder were collected over a 2θ range of 35–70° at a scan rate of 0.3° 2θ/min. The mass loss of the samples as a function of temperature was monitored with a NETZSCH STA 409 PC/PG TGA (Selb, Germany), at a heating rate of 10 °C/min, under nitrogen atmosphere from 50 to 900 °C. The FTIR spectra of the lyophilized samples were recorded using a JASCO Corp., FT/IR-420 (Tokyo, Japan); over a spectral range of 400–4000 cm^{-1}. The Raman spectrum of the synthesized nanoparticles was recorded at room temperature using the 532 nm line from a diode laser (SUWTECH, G-SLM, Shanghai, China). The scattered light was collected and detected using a CCD based monochromator, covering a spectral range of 150–1700 cm^{-1}. The sample solution was taken in a standard 1 cm × 1 cm cuvette and placed in the path of the laser beam. The zeta potential of the nanoparticle solutions was measured with a Malvern Zetasizer Nanosystem (Worcestershire, UK).

2.3. Antibacterial assay

The well diffusion method was used to study the antibacterial activity of the synthesized silver nanoparticles (Kora, Manjusha, & Arunachalam, 2009). All the glassware, media and reagents used were sterilized in an autoclave at 121 °C for 20 min. *Staphylococcus aureus* (ATCC 25923); and *Escherichia coli* (ATCC 25922), *E. coli* (ATCC 35218) and *Pseudomonas aeruginosa* (ATCC 27853) were used as model test strains for Gram-positive and Gram-negative bacteria, respectively. Bacterial suspension was prepared by growing a single colony overnight in nutrient broth and by adjusting the turbidity to 0.5 McFarland standards (Kora et al., 2009). Mueller Hinton agar (MHA) plates were inoculated with this bacterial suspension and 5 μg of silver nanoparticles were added to the center well with a diameter of 8 mm. The nanoparticles used here were prepared with 0.5% (w/v) gum KG solution containing 1 mM $AgNO_3$, autoclaved for 60 min. Control plates were maintained with autoclaved gum loaded wells. These plates were incubated at 37 °C for 24 h in a bacteriological incubator and the zone of inhibition (ZOI) was measured by subtracting the well diameter from the total inhibition zone diameter. Three independent experiments were carried out with each strain.

3. Results and discussion

3.1. Synthesis of silver nanoparticles

The present experimental investigation reports the green synthesis of silver nanoparticles using gum kondagogu by autoclaving. This method utilizes a non-toxic, renewable gum kondagogu which

functions as both reducing and stabilizing agent during synthesis. By virtue of being a natural polymer, this gum is also amenable for biodegradation. The process of autoclaving makes the silver nanoparticles intrinsically safe and sterile, in environmentally benign solvent water. Moreover, generation of gum-silver nanoparticles by autoclaving is a prerequisite for microbiological applications. Thus, the adopted method is meeting the requirements of green chemistry principles.

3.1.1. Proposed mechanism of reduction

During autoclaving at 121 °C under the influence of temperature and pressure, this biopolymer expands and becomes more accessible for the silver ions to interact with the available functional groups on the gum, as observed earlier for starch (Vigneshwaran et al., 2006). The gum has been categorized under rhamnogalacturonans due to the abundance of rhamnose, galactose and uronic acids (Vinod & Sashidhar, 2009; Vinod, Sashidhar, Sarma, & Saradhi, 2008). Earlier characterization studies established the abundance of hydroxyl, carbonyl and carboxylic functional groups in this gum. This gum is known to be rich in uronic acid content and shows a pH of 4.9–5.0. The presence of negatively charged groups is also confirmed from the negative zeta potential value of −23.4 mV for the gum (Vinod, Sashidhar, Sreedhar, et al., 2009; Vinod, Sashidhar, & Sukumar, 2009). The large number of hydroxyl and carboxylic groups on this biopolymer facilitates the complexation of silver ions. Subsequently, these silver ions oxidize the hydroxyl groups to carbonyl groups, during which the silver ions are reduced to elemental silver. In addition to this inherent oxidation, the dissolved air also causes oxidation of the existing hydroxyl groups to carbonyl groups such as aldehydes and carboxylates. In turn, these powerful reducing aldehyde groups along with the other existing abundant carbonyl groups reduce more and more of silver ions to elemental silver. Further, these nanoparticles are probably capped and stabilized by the polysaccharides along with the proteins present in the gum. As these carbohydrate polymers are very complex, it is most likely that more than one mechanism is involved in the complexation and subsequent reduction of silver ions by gum kondagogu during autoclaving. It is reported that the hydroxyl and carboxylate functional groups of gum kondagogu are involved in cadmium biosorption (Vinod, Sashidhar, Sreedhar, et al., 2009). Silver ion complexation by hydroxyl groups and its subsequent reduction by aldehyde groups are reported for starch, in which silver nanoparticles were produced by autoclaving (Vigneshwaran et al., 2006). Silver nanoparticles produced using gum Acacia, carboxylate groups involving complexation of silver ions and its subsequent reduction by hydroxyl groups were reported (Mohan et al., 2007). In previous studies carried out with PEG (Luo et al., 2005), PVP (Xiong et al., 2006), Apiin (Kasthuri, Veerapandian, & Rajendiran, 2009); and alginate (Pal et al., 2005), hydroxyl group mediated reduction was reported for the synthesis of silver and gold nanoparticles.

The reduction of silver ions by this gum even at room temperature was observed. But the formed nanoparticles were not stable and aggregated due to lack of stabilization of the synthesized nanoparticles. It was noticed that the autoclaving at 121 °C and 15 psi of pressure, increased the extent of synthesis and stabilization of the nanoparticles. It is known that elevated temperature and pressure accelerate the synthesis of nanoparticles (Vigneshwaran et al., 2006). Besides, this process complexly eliminates the microbial contamination such as bacteria, viruses and spores from gum kondagogu which were possibly acquired during gum secretion, collection and transportation.

3.2. Characterization of synthesized silver nanoparticles

3.2.1. UV–visible spectroscopy (UV–vis)

The UV–visible absorption spectroscopy is one of the most widely used simple and sensitive techniques for the observation of nanoparticle synthesis. In order to monitor the formation of silver nanoparticles, the absorption spectra of synthesized silver nanoparticles were recorded against respective autoclaved gum blanks. Fig. 1 is indicating (a) gum tears of grade 1 quality, (b) gum powder sieved to 38 μm particle size and (c) gum solution of 0.5% (w/v). After autoclaving the gum solutions containing silver nitrate, the appearance of yellow colour in the reaction mixtures was observed. (For interpretation of the references to colour in this sentence, the reader is referred to the web version of the article.) This is a clear indication for the formation of silver nanoparticles by the gum [inset of Fig. 2(b)]. To optimize the nanoparticle synthesis, the influence of different parameters such as gum particle size, concentration of gum, concentration of silver nitrate and reaction time was studied. The role of particle size of the gum on the synthesis was studied with 0.5% solutions prepared with powders of gum sieved to 300, 105 and 38 μm. This reaction was carried out by autoclaving these gum solutions containing 1 mM of silver nitrate for 20 min. As the particle size decreases to 38 μm, the absorbance intensity of the solutions was found to increase. This increase in absorbance can be attributed to an increase in the surface area of the gum particles and the extent of gum dissolution [Fig. 2(a)]. Further experiments were carried out using the gum solution obtained with 38 μm sized gum. Fig. 2(b) shows the UV–vis spectra of the produced silver nanoparticles with different concentrations of gum (0.1–0.5%) at 1 mM $AgNO_3$ and 20 min of autoclaving. It reveals that the efficiency of nanoparticle synthesis increases with increasing concentration of gum. Fig. 2(b) (inset) indicates the increased colour intensity of the nanoparticle solution with increase in gum concentration. Fur-

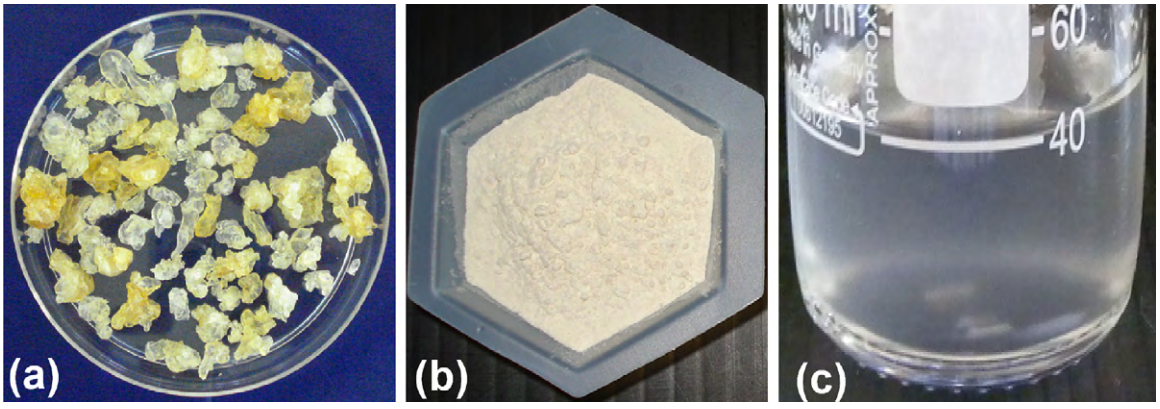

Fig. 1. (a) Gum tears of grade 1 quality, (b) gum powder sieved to 38 μm particle size and (c) gum solution of 0.5% (w/v).

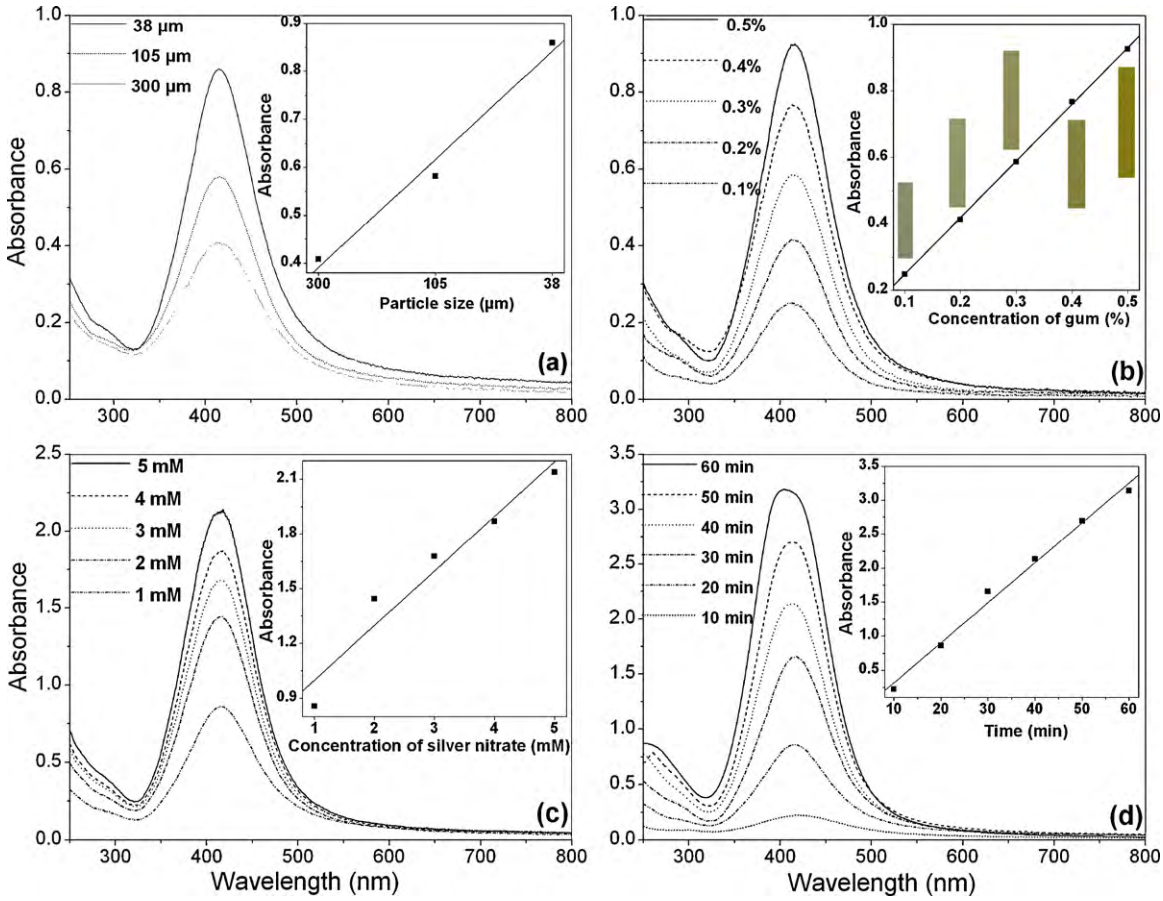

Fig. 2. The UV–vis absorption spectra of silver nanoparticles synthesized: (a) with 0.5% (w/v) gum solutions containing 1 mM $AgNO_3$, using KG sieved to 300, 105 and 38 µm particle size by autoclaving for 20 min; inset plot of A_{max} *versus* gum particle size, (b) by autoclaving different concentrations of gum KG solutions at 1 mM $AgNO_3$ concentration for 20 min; inset plot of A_{max} *versus* gum concentration, indicating the progressive colour intensity of the solutions, (c) by autoclaving different concentrations of $AgNO_3$ solutions at 0.5% (w/v) gum KG for 20 min; inset plot of A_{max} *versus* $AgNO_3$ concentration and (d) with 0.5% (w/v) gum KG solutions at 1 mM $AgNO_3$ concentration for different durations of autoclaving; inset plot of A_{max} *versus* autoclaving time.

ther, the production of nanoparticles with 0.5% gum was monitored with varying concentrations of silver nitrate for 20 min of reaction time and their respective spectra are depicted in Fig. 2(c). The absorbance intensity of the solutions increased with higher concentrations of silver nitrate due to an enhancement in the oxidation of hydroxyl groups by silver ions. The synthesis was also evaluated by varying the reaction time (10–60 min) and reduction was studied with 0.5% gum at 1 mM $AgNO_3$ [Fig. 2(d)]. It was noticed that the reduction capacity of the gum increased with reaction time. As the autoclaving time increases, possibly more and more of hydroxyl groups are being converted to carbonyl groups by air oxidation, which in turn reduce the silver ions. In the UV–vis spectra a single strong peak with a maximum around 416 nm was observed, which corresponds to the typical surface plasmon resonance (SPR) of conducting electrons from the surface of silver nanoparticles (Kora et al., 2009). In all these spectra, there are no peaks located around 335 and 560 nm, indicating the complete absence of nanoparticle aggregation (Kora et al., 2009; Mohan et al., 2007).

3.2.2. Transmission electron microscopy (TEM)

Figs. 3 and 4 show the TEM images of the silver nanoparticles synthesized with 0.1% gum KG and 1 mM $AgNO_3$, autoclaved for 30 and 60 min, respectively. The TEM observations of the samples indicate the shape anisotropy and the nanoparticles display a rich variety of shapes in varying sizes. In addition to nanospheres, some pronounced anisotropic nanostructures such as nanotriangles, a few nanorods, hexagonal and polygonal nanoprisms; and abundant uneven shaped nanoparticles were observed (Appendix A). These nanoparticles are polydisperse and the average particle sizes obtained from these micrographs were about 55.0 and 18.9 nm, respectively [Figs. 3(d) and 4(d)], for 30 and 60 min of reaction time. The selected-area electron diffraction (SAED) patterns depicted in Figs. 3(c) and 4(c) exhibit concentric rings with intermittent bright dots, indicating that these nanoparticles are highly crystalline in nature. These rings can be attributed to the diffraction from the (1 1 1), (2 0 0), (2 2 0) and (3 1 1) planes of face centered cubic (fcc) silver. The crystallinity of the synthesized nanoparticles was also supported from the observed clear lattice fringes of around 0.24 nm in high-resolution images [Fig. 3(b) and 4(b)]. The morphology of the nanoparticles synthesized with 0.5% gum KG and 1 mM $AgNO_3$, autoclaved for 30 and 60 min, respectively, were also confirmed with TEM (Fig. 5). These silver nanoparticles were observed to be spherical in shape and well separated in aqueous medium. The average particle sizes obtained from the corresponding diameter distributions were about 11.2 and 4.5 nm [Fig. 5(b) and (d)]. Interestingly with 60 min of autoclaving, nearly 70% of the nanoparticles formed were in the size of 3 nm [Fig. 5(c)]. When the concentration of gum was increased from 0.1 to 0.5%, the particle size of the silver nanoparticles formed decreased. These findings are similar to the one reported earlier for gum Acacia (Mohan et al., 2007). This was also confirmed in a previous study on biosynthesis of gold nanoparticles with sodium alginate, in which the concentration of the biopolymer increased from 0.01 to 0.1% (Pal et al., 2005). The decrease in anisotropy and polydispersity with increase in the concentration of gum was also evident from the TEM images. It is worth noting that the shape of the particles changed from

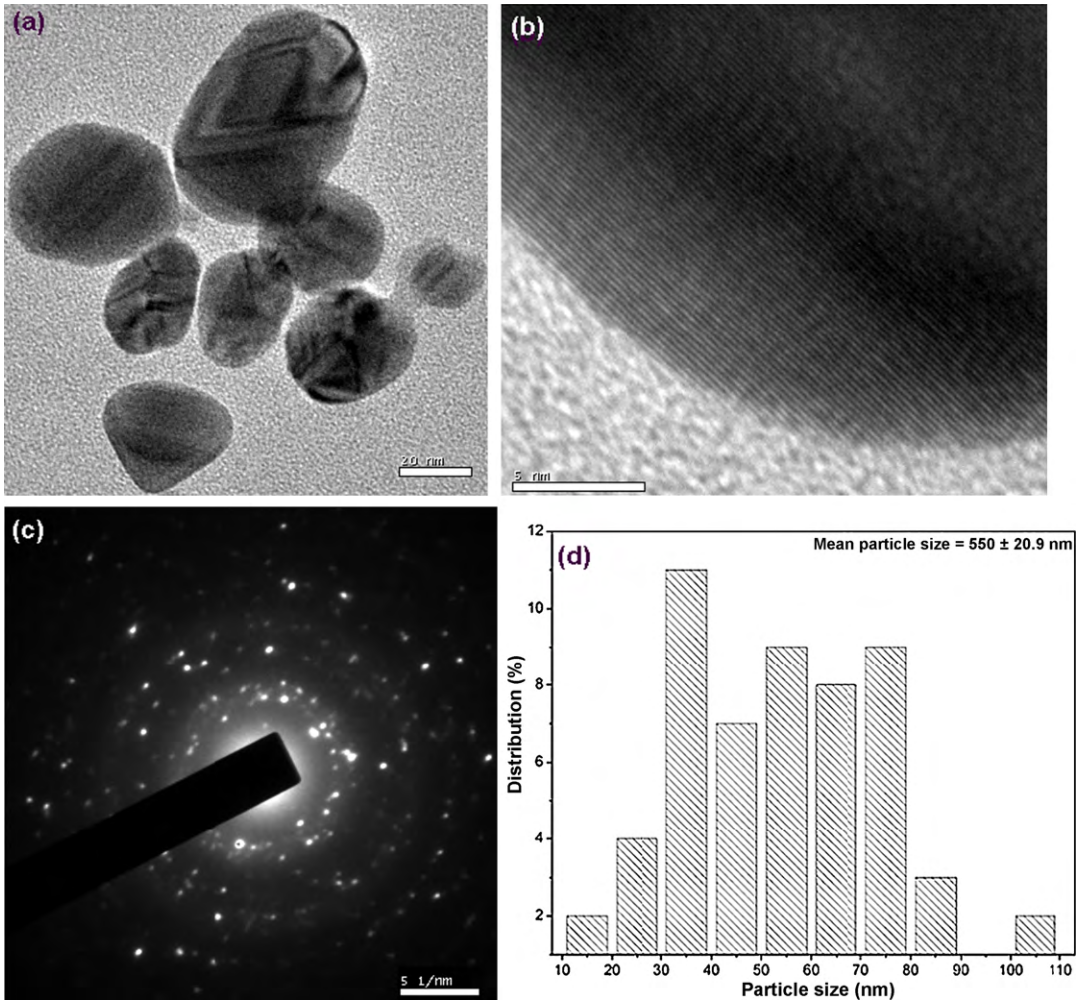

Fig. 3. (a) TEM image of silver nanoparticles synthesized with 0.1% (w/v) gum KG and 1 mM $AgNO_3$, autoclaved for 30 min, (b) high-resolution image of a single particle, (c) corresponding SAED pattern and (d) histogram showing the particle size distribution.

anisotropic nanostructures to spheres, when the concentration of gum is increased to 0.5%. This was also established in a previous study on biological synthesis of gold nanoparticles with Apiin, a glycoside extracted from the leaves of *Henna* (Kasthuri et al., 2009). This study indicates that the particle size of the silver nanoparticles can be controlled by varying the concentration of gum and reaction time. At higher gum concentration, the interaction between ionic silver and function groups on gum as well as the rate of nanoparticle capping were excellent. In addition, the aggregation was lower due to lesser collisions of silver nanoparticles. As a result, nanoparticles with monodispersity were obtained with 0.5% gum and 60 min of reaction time at 1 mM of silver nitrate concentration.

3.2.3. X-ray diffraction (XRD)

The XRD technique was used to determine and confirm the crystal structure of silver nanoparticles. As the nanoparticles are within the gum matrix, the diffraction intensity of the silver was low (data not shown). Hence, the lyophilized nanoparticle sample was calcined at 400 °C to remove the high noise originating from the gum and the XRD pattern is shown in Fig. 6(a). As expected, the XRD peaks were much stronger and sharper as compared to the non-calcined sample possibly due to the removal of noisy background and the growth of crystallites. There were three well-defined characteristic diffraction peaks at 38.3°, 44.2° and 64.5°, respectively, corresponding to (1 1 1), (2 0 0) and (2 2 0) planes of face centered cubic (fcc) crystal structure of metallic silver. The interplanar spacing (d_{hkl}) values (2.352, 2.048 and 1.447 Å) calculated from the XRD spectrum of silver nanoparticles are agreeing well with the standard silver values. Thus, the XRD pattern, further corroborating the highly crystalline nature of nanoparticles observed from SAED patterns and high-resolution TEM images (Figs. 3 and 4). The broadening of the diffraction peaks was observed owing to the effect of nano-sized particles. The lattice constant calculated from this pattern was 4.088 Å, a value which is in agreement with the value reported in literature for silver (a = 4.086 Å; JCPDS PDF 04-0783). As indicated in Fig. 6(a), the highly intense diffraction peak is located at 38.3° and the peaks at (2 0 0) and (2 2 0) planes are less intense. It is worth pointing that the ratio of the intensity between (2 0 0) and (1 1 1) peaks is much lower than the standard value (0.1 *versus* 0.4). In addition, the ratio between (2 2 0) and (1 1 1) peaks is also lower than the standard value (0.14 *versus* 0.25). These results clearly demonstrate that the (1 1 1) lattice plane is the preferred orientation for the calcined silver nanoparticles. Our experimental findings are in concurrence with the observations reported by other researchers (Kora et al., 2009).

3.2.4. Thermogravimetric analysis (TGA)

The thermal stability of the gum-silver nanoparticles and the gum was monitored by TGA and the thermograms are given in Fig. 6(b). Both the samples show three successive weight losses in the temperature region 50–900 °C. The initial weight loss observed was attributed to loss of bound water molecules from the poly-

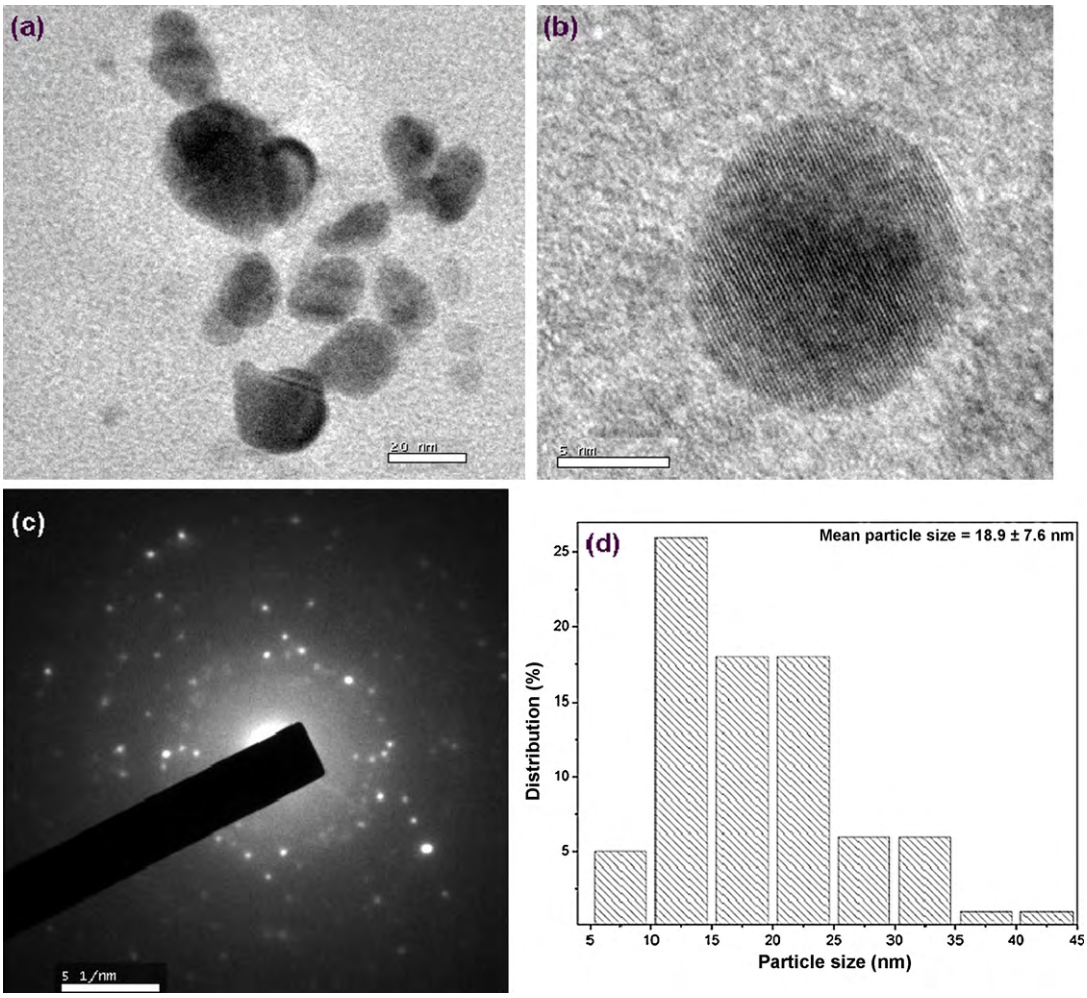

Fig. 4. (a) TEM image of silver nanoparticles synthesized with 0.1% (w/v) gum KG and 1 mM $AgNO_3$, autoclaved for 60 min, (b) high-resolution image of a single particle, (c) corresponding SAED pattern and (d) histogram showing the particle size distribution.

mer matrix. The second step is most likely the consequence of the thermal degradation of the polymer as well as the polymer capping around the nanoparticles (Kasthuri et al., 2009). While, the third weight loss could be due to the conversion of remaining polymer to carbon residue. The thermal degradation pattern observed for the gum is in concurrence with studies carried out by earlier researchers (Naidu et al., 2009; Vinod & Sashidhar, 2009). A low percent weight loss was noticed for the gum after nanoparticle synthesis compared to before synthesis. 32.32% of the initial weight was found to be retained for gum-nanoparticles against 20.57% for gum at 900 °C. These findings reveal the better thermal stability of the gum-silver nanoparticles over the gum alone (Reddy et al., 2008).

3.2.5. Fourier transform infrared spectroscopy (FTIR)

The FTIR spectra of the gum-nanoparticles and gum were recorded in order to identify the functional groups of gum involved in the reduction of the synthesized nanoparticles. Fig. 7(a) shows the FTIR spectra of the gum before and after nanoparticle formation. The major absorbance bands present in the spectrum of gum kondagogu were at 3455, 2918, 2851, 1735, 1631, 1601, 1384, 1384, 1352, 1254, 1151 and 1045 cm^{-1}, respectively. While, the spectrum of gum-nanoparticles showed characteristic absorbance bands at 3443, 2916, 2850, 1727, 1630, 1597, 1384, 1351, 1254, 1148 and 1043 cm^{-1}, respectively. The broad band observed at 3443 cm^{-1} could be assigned to stretching vibration of O–H groups. The bands at 2916 and 2850 cm^{-1} correspond to asymmetric and symmetric C–H stretch, respectively. The peak at 1727 cm^{-1} arises from the carbonyl stretching vibrations. The stronger bands found at 1630 and 1597 cm^{-1} could be assigned to characteristic asymmetrical stretch of carboxylate group. The symmetrical stretch of carboxylate group can be attributed to the bands present at 1384 and 1351 cm^{-1}. The peak at 1254 cm^{-1} indicates the acetyl group. The peaks at 1148 and 1043 cm^{-1} were due to the C–O stretching vibration of ether and alcoholic groups, respectively. After autoclaving, a shift in absorbance peak was observed from 3455 to 3443 cm^{-1} with increased band intensity, suggesting the binding of silver ions with hydroxyl groups. Further, predominantly the band intensities of carboxylate groups were found to be enhanced after autoclaving the gum, indicative of more extensively oxidized nature of the gum. The band shift in the hydroxyl groups and increased band intensities for carbonyl groups in FTIR spectra confirm the oxidation of these functional groups during autoclaving. Based on this evidence, it can be inferred that both hydroxyl and carbonyl groups of gum are involved in the synthesis of silver nanoparticles. The variations in the shape and peak position of the hydroxyl and carboxylate groups have been reported, where silver nanoparticles were synthesized using another polysaccharide, gum Acacia (Mohan et al., 2007).

3.2.6. Raman spectroscopy

In order to find out the possible functional groups of capping agents associated in the stabilization of silver nanoparticles, Raman spectrum of the nanoparticles was recorded. Fig. 7(b) gives

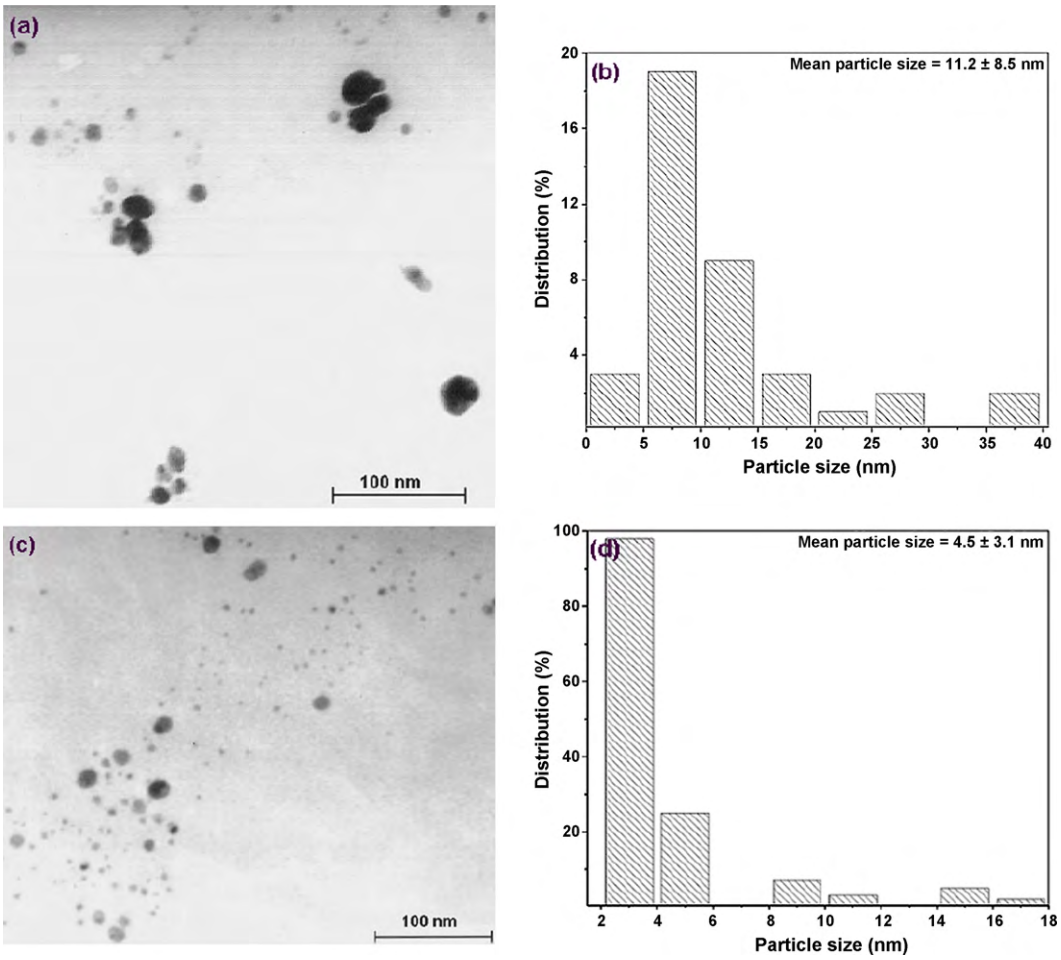

Fig. 5. (a) TEM image of silver nanoparticles synthesized with 0.5% (w/v) gum KG and 1 mM $AgNO_3$, autoclaved for 30 min, (b) histogram showing the particle size distribution, (c) TEM image of silver nanoparticles synthesized with 0.5% (w/v) gum KG and 1 mM $AgNO_3$, autoclaved for 60 min and (d) histogram showing the particle size distribution.

the selective enhancement of Raman bands of the organic capping agents bound to the nanoparticles. The spectrum shows a strong and sharp band at 241 cm^{-1}, which can be attributed to the stretching vibrations of Ag–N (Chowdhury & Ghosh, 2004; Mukherjee et al., 2008) and Ag–O bonds (Biswas, Kapoor, Mahal, & Mukherjee, 2007). This peak indicates the formation of a chemical bond between silver and amino nitrogen (Mukherjee et al., 2008); and silver and carboxylate groups (Biswas et al., 2007) of gum molecules. It confirms that the gum is bound to the silver nanoparticle surface either through amino or carboxylate group or both. It is known to have close frequencies for the Ag–N and Ag–O stretching vibrations and the involvement of both N and O atoms in binding result in SERS band broadening (Chowdhury & Ghosh, 2004). The broad ones at 1350 and 1548 cm^{-1} correspond to symmetric and asymmetric C=O stretching vibrations of carboxylate group, respectively (Mukherjee et al., 2008). The enhancement in the intensity of the CO_2 stretching vibration suggests the direct binding of the COO^- group with the silver surface (Biswas et al., 2007). The sharp peak at 1123 cm^{-1} comes from the C–H in plane bending (Chowdhury & Ghosh, 2004) of the saccharide structure of gum. Thus, from the preferential enhancement of these bands; it can be concluded that both amino and carboxylate groups of the gum are involved in the capping of the silver nanoparticles. These results are in concurrence with earlier biosynthesis of silver nanoparticles carried out with non-pathogenic fungus *Trichoderma asperellum* (Mukherjee et al., 2008). It was reported earlier that the carboxylate groups of glycoprotein of gum Acacia were involved in binding of silver nanoparticles (Mohan et al., 2007). It is known that proteins can bind to nanoparticles either through free amino groups or by electrostatic interaction of negatively charged carboxylate groups (Vigneshwaran et al., 2007). The gum kondagogu is known to contain higher amount of protein and the protein content was reported to be in the range of 5–6.3% (Janaki & Sashidhar, 1998). This observation is further substantiated by the UV–vis absorption spectrum of the 0.5% (w/v) gum solution against water blank given in the inset of Fig. 7(b). An absorption peak at 280 nm is clearly visible and is attributed to electronic excitations in tryptophan and tyrosine residues in the proteins (Vigneshwaran et al., 2007), which are present in the gum. Being rich in uronic acid content, the presence of negatively charged groups is also confirmed from the zeta potential value of −23.4 mV for the gum (Vinod, Sashidhar, Sreedhar, et al., 2009). Thus, one can conclude that once the silver ions are reduced to silver nanoparticles by the polyhydroxylated gum, proteins present in the gum subsequently encapsulate and stabilize these particles along with saccharide molecules. Based on these observations, these silver nanoparticles can be used as a possible substrate for surface-enhanced Raman scattering (SERS).

As mentioned above, gum kondagogu is rich in various functional groups; and their capping on silver nanoparticles provides surface reactivity. It is reported that the functional unit used as a capping agent plays an important role and determines the tissue distribution profile of gold nanoparticles (Fent et al., 2009). Thus, these functionalized nanoparticles are useful for various applications such as drug delivery (Dhar et al., 2008), biological labels (Schrand, Braydich-Stolle, Schlager, Dai, & Hussain, 2008) and targeted biological interactions (Fent et al., 2009). In addi-

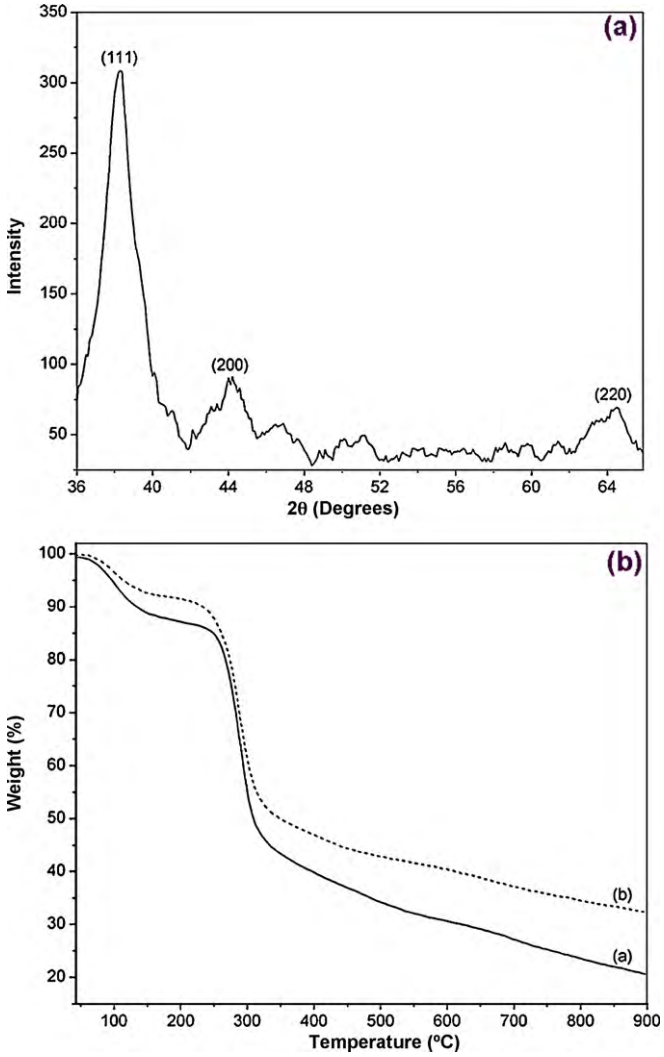

Fig. 6. (a) X-ray diffraction pattern of silver nanoparticles calcined at 400 °C and (b) thermogravimetric analysis of freeze dried (a) gum kondagogu and (b) gum kondagogu-silver nanoparticles.

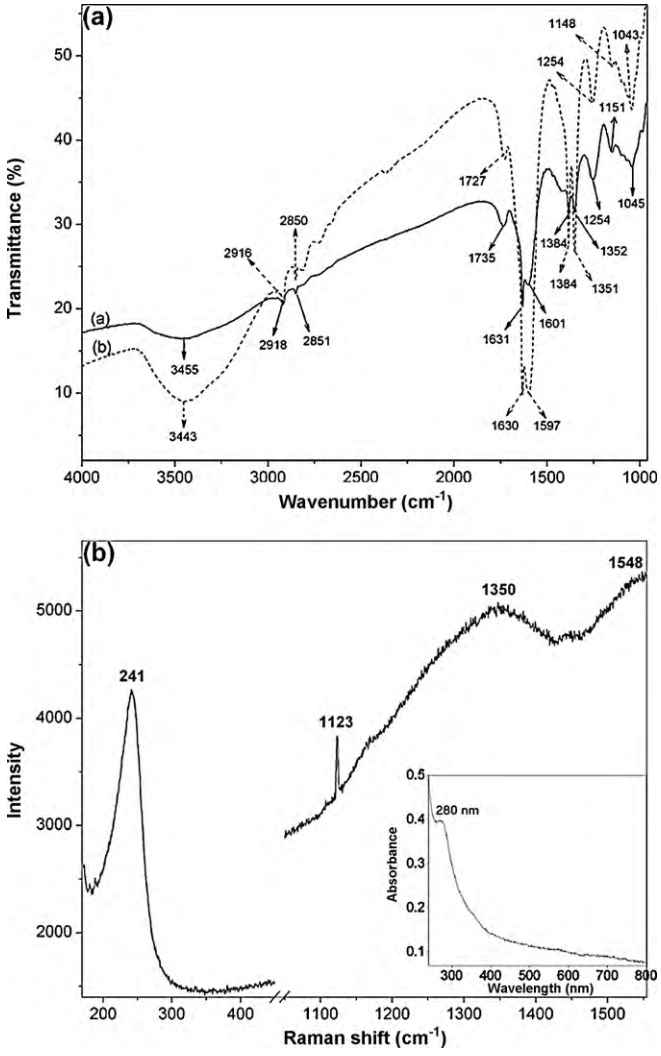

Fig. 7. (a) FTIR spectra of freeze dried (a) gum kondagogu and (b) gum kondagogu-silver nanoparticles and (b) Raman spectrum of aqueous silver nanoparticle solution. Inset: the UV–vis absorption spectrum of the 0.5% (w/v) gum solution against water blank.

tion, the solutions of silver nanoparticles are clear yellow, without any colour change and visual aggregation for more than a year. This observation is also validated with the recorded zeta potential value of −30.3 mV for the nanoparticles prepared with 0.5% gum and 60 min of reaction time at 1 mM of silver nitrate. Besides, the absorbance spectra of silver nanoparticles showed hardly any change in the λ_{max} and intensity values, even after one year of storage. This observation is supported by the complete absence of peaks at 335 and 560 nm in UV–vis absorption spectra, indicating no nanoparticle aggregation or nanocluster formation (Fig. 2) (Kora et al., 2009; Mohan et al., 2007). Hence, silver nanoparticles formed by this method are highly stable and well dispersed in nature.

3.3. Antibacterial assay

For checking the antibacterial activity, silver nanoparticles with an average size of 4.5 nm were used. These nanoparticles were prepared with 0.5% gum KG solution containing 1 mM $AgNO_3$, autoclaved for 60 min. After 24 h of incubation at 37 °C, growth suppression was observed in plates loaded with 5 μg of silver nanoparticles. Whereas, the control plate loaded with autoclaved gum did not produce any ZOI (Fig. 8). Bacterial growth inhibition around the well is due to the release of diffusible inhibitory compounds from silver nanoparticles. The ZOI of around 11 mm was observed for the Gram-positive bacterial strain *S. aureus* ATCC 25923. In the case of Gram-negative bacterial strains *E. coli* ATCC 25922, *E. coli* ATCC 35218 and *P. aeruginosa* ATCC 27853; the detected ZOI were 8.0, 8.4 and 8.7 mm, respectively. Based on these results, it can be concluded that synthesized silver nanoparticles had significant antibacterial action on both the Gram classes of bacteria.

In the present study, a higher inhibition zone was observed for the Gram-positive *S. aureus* compared to other Gram-negative strains employed in this antibacterial susceptibility assay. This observation is in excellent agreement with earlier studies (Cho et al., 2005; Sharma et al., 2009; Xu et al., 2006, 2009). It was earlier reported that the antibacterial activity of the nanoparticles is directly proportional to the zeta potential (Du, Niu, Xu, Xu, & Fan, 2009). The zeta potential value of the silver nanoparticles used in the present assay was found to be −30.3 mV. The differential sensitivity of Gram-negative and Gram-positive bacteria towards silver nanoparticles possibly depends upon their cell surface characteristics and their interaction with the charged gum-silver nanoparticles. It was observed that the negative charge on the cell surface of Gram-negative bacteria was higher than that on Gram-positive bacteria (Chung et al., 2004). Consequently, the

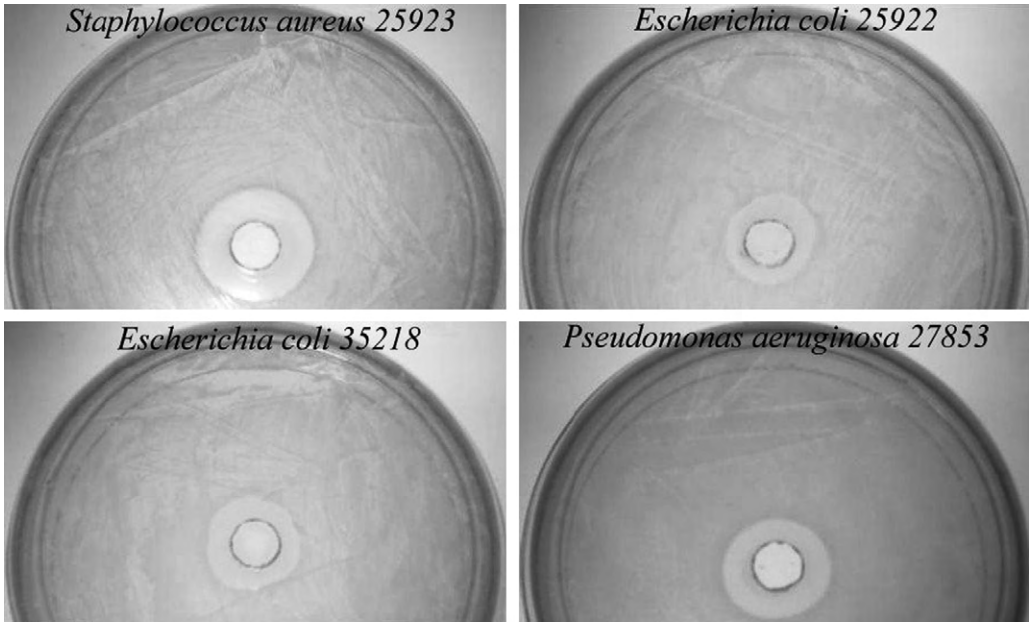

Fig. 8. Bacterial culture plates showing the inhibition zones around wells loaded with 5 μg of silver nanoparticles (0.5% (w/v) gum KG, 1 mM $AgNO_3$ and 60 min).

interaction between Gram-positive bacteria and silver nanoparticles was certainly stronger than that of Gram-negative bacteria. Besides, the cell wall of Gram-negative bacteria consists of an outer membrane composed of lipids, proteins and lipopolysaccharides (LPS) which act as a barrier and provide effective protection against antibacterial agents. But the cell walls of Gram-positive bacteria do not consist of an outer membrane (Maneerung et al., 2008; Xu et al., 2006).

4. Conclusions

The present study reports the facile synthesis of silver nanoparticles from silver nitrate using gum kondagogu as a template. The adopted method is compatible with green chemistry principles as the gum serves as a matrix for both reduction and stabilization of the silver nanoparticles synthesized. At a given gum concentration, the efficiency of nanoparticle synthesis increases with silver nitrate concentration and reaction time, a property attributable to the large reduction capacity of the gum. As the particle size of the nanoparticles can be controlled, this method can be implemented for the large scale production of monodispersed and spherical nanoparticles of around 3 nm due to the availability of low cost plant derived biopolymer. The abundance of hydroxyl and carboxylate groups facilitates the complexation of silver ions during autoclaving. Subsequently, these silver ions are reduced to elemental silver possibly by *in situ* oxidation of hydroxyl groups; and by the intrinsic carbonyl groups as well as those produced by the air oxidation. This proposed mechanism is also substantiated by the FTIR data. Further, these metal nanoparticles were found to enhance the thermal stability of the gum. The formed silver nanoparticles are highly stable and had significant antibacterial action on both the Gram classes of bacteria. The surface reactivity facilitated by capping enables these functionalized nanoparticles as promising candidates for various pharmaceutical, biomedical and environmental applications. Notably, selective enhancement of Raman bands of the organic capping agents bound to the silver colloids facilitates these nanoparticles as suitable substrates for SERS. In view of this, further studies are envisaged to explore the other potential applications of this gum based nanoparticles.

Acknowledgements

We thank Dr. S.V. Narasimhan, Associate Director and Dr. Tulsi Mukherjee, Director, Chemistry Group, BARC for their constant support and encouragement for this work. The support rendered for high-resolution TEM measurements by the DST unit on Nanoscience, Sophisticated Analytical Instrument Facility (SAIF) at IIT-Madras, Chennai is gratefully acknowledged.

Appendix A. Supplementary data

Supplementary data associated with this article can be found, in the online version, at doi:10.1016/j.carbpol.2010.05.034.

References

Biswas, N., Kapoor, S., Mahal, H. S., & Mukherjee, T. (2007). Adsorption of CGA on colloidal silver particles: DFT and SERS study. *Chemical Physics Letters*, *444*, 338–345.

Cho, K. H., Park, J. E., Osaka, T., & Park, S. G. (2005). The study of antimicrobial activity and preservative effects of nanosilver ingredient. *Electrochimica Acta*, *51*, 956–960.

Chowdhury, J., & Ghosh, M. (2004). Concentration-dependent surface-enhanced Raman scattering of 2-benzoylpyridine adsorbed on colloidal silver particles. *Journal of Colloid and Interface Science*, *277*, 121–127.

Chung, Y. C., Su, Y. P., Chen, C. C., Jia, G., Wang, H. L., Wu, J. C. G., et al. (2004). Relationship between antibacterial activity of chitosan and surface characteristics of cell wall. *Acta Pharmacologica Sinica*, *25*, 932–936.

Dhar, S., Reddy, E. M., Shiras, A., Pokharkar, V., & Prasad, B. L. V. (2008). Natural gum reduced/stabilized gold nanoparticles for drug delivery formulations. *Chemistry A European Journal*, *14*, 10244–10250.

Du, W. L., Niu, S. S., Xu, Y. L., Xu, Z. R., & Fan, C. L. (2009). Antibacterial activity of chitosan tripolyphosphate nanoparticles loaded with various metal ions. *Carbohydrate Polymers*, *75*, 385–389.

Fent, G. M., Casteel, S. W., Kim, D. Y., Kannan, R., Katti, K., Chanda, N., et al. (2009). Biodistribution of maltose and gum arabic hybrid gold nanoparticles after intravenous injection in juvenile swine. *Nanomedicine: Nanotechnology, Biology, and Medicine*, *5*, 128–135.

Huang, H., & Yang, X. (2004). Synthesis of polysaccharide-stabilized gold and silver nanoparticles: A green method. *Carbohydrate Research*, *339*, 2627–2631.

Inoue, Y., Hoshino, M., Takahashi, H., Noguchi, T., Murata, T., Kanzaki, Y., et al. (2002). Bactericidal activity of Ag-zeolite mediated by reactive oxygen species under aerated conditions. *Journal of Inorganic Biochemistry*, *92*, 37–42.

Janaki, B., & Sashidhar, R. B. (1998). Physico-chemical analysis of gum kondagogu (*Cochlospermum gossypium*): A potential food additive. *Food Chemistry*, *61*, 231–236.

Janaki, B., & Sashidhar, R. B. (2000). Sub chronic (90-day) toxicity study in rats fed gum Kondagogu (*Cochlospermum gossypium*). *Food and Chemical Toxicology*, *38*, 523–534.

Jonathan, C. R., Amanda, J. H., Adam, D. M., Chanda, R. Y., & Richard, P. V. D. (2003). A nanoscale optical biosensor: Real-time immunoassay in physiological buffer enabled by improved nanoparticle adhesion. *Journal of Physical Chemistry B*, *107*, 1772–1780.

Kasthuri, J., Veerapandian, S., & Rajendiran, N. (2009). Biological synthesis of silver and gold nanoparticles using apiin as reducing agent. *Colloids and Surfaces B: Biointerfaces*, *68*, 55–60.

Kora, A. J., Manjusha, R., & Arunachalam, J. (2009). Superior bactericidal activity of SDS capped silver nanoparticles: Synthesis and characterization. *Materials Science and Engineering C*, *29*, 2104–2109.

Luo, C., Zhang, Y., Zeng, X., Zeng, Y., & Wang, Y. (2005). The role of poly(ethylene glycol) in the formation of silver nanoparticles. *Journal of Colloid and Interface Science*, *288*, 444–448.

Mahapatra, S. S., & Karak, N. (2008). Silver nanoparticle in hyperbranched polyamine: Synthesis, characterization and antibacterial activity. *Materials Chemistry and Physics*, *112*, 1114–1119.

Maneerung, T., Tokura, S., & Rujiravanit, R. (2008). Impregnation of silver nanoparticles into bacterial cellulose for antimicrobial wound dressing. *Carbohydrate Polymers*, *72*, 43–51.

Mohan, Y. M., Raju, K. M., Sambasivudu, K., Singh, S., & Sreedhar, B. (2007). Preparation of Acacia-stabilized silver nanoparticles: A green approach. *Journal of Applied Polymer Science*, *106*, 3375–3381.

Mukherjee, P., Roy, M., Mandal, B. P., Dey, G. K., Mukherjee, P. K., Ghatak, J., et al. (2008). Green synthesis of highly stabilized nanocrystalline silver particles by a non-pathogenic and agriculturally important fungus *T. asperellum*. *Nanotechnology*, *19*, 075103–075110.

Naidu, V. G. M., Madhusudhana, K., Sashidhar, R. B., Ramakrishna, S., Khar, R. K., Ahmed, F. J., et al. (2009). Polyelectrolyte complexes of gum kondagogu and chitosan, as diclofenac carriers. *Carbohydrate Polymers*, *76*, 464–471.

Pal, A., Esumi, K., & Pal, T. (2005). Preparation of nanosized gold particles in a biopolymer using UV photoactivation. *Journal of Colloid and Interface Science*, *288*, 396–401.

Reddy, K. R., Lee, K., Lee, Y., & Gopalan, A. I. (2008). Facile synthesis of conducting polymer–metal hybrid nanocomposites by in situ chemical oxidative polymerization with negatively charged metal nanoparticles. *Materials Letters*, *62*, 1815–1818.

Schrand, A. M., Braydich-Stolle, L. K., Schlager, J. J., Dai, L., & Hussain, S. M. (2008). Can silver nanoparticles be useful as potential biological labels? *Nanotechnology*, *19*, 235104–235116.

Sharma, V. K., Yngard, R. A., & Lin, Y. (2009). Silver nanoparticles: Green synthesis and their antimicrobial activities. *Advances in Colloid and Interface Science*, *145*, 83–96.

Tien, D., Tseng, K., Liao, C., & Tsung, T. (2009). Identification and quantification of ionic silver from colloidal silver prepared by electric spark discharge system and its antimicrobial potency study. *Journal of Alloys and Compounds*, *473*, 298–302.

Tiwari, D. K., Behari, J., & Sen, P. (2008). Time and dose-dependent antimicrobial potential of Ag nanoparticles synthesized by top-down approach. *Current Science*, *95*, 647–655.

Totaro, P., & Rambaldini, M. (2009). Efficacy of antimicrobial activity of slow release silver nanoparticles dressing in post-cardiac surgery mediastinitis. *Interactive Cardiovascular and Thoracic Surgery*, *8*, 153–154.

Vegi, G. M. N., Sistla, R., Srinivasan, P., Beedu, S. R., Khar, R. K., & Diwan, P. V. (2009). Emulsifying properties of gum kondagogu (*Cochlospermum gossypium*), a natural biopolymer. *Journal of the Science of Food and Agriculture*, *89*, 1271–1276.

Vigneshwaran, N., Ashtaputre, N. M., Varadarajan, P. V., Nachane, R. P., Paralikar, K. M., & Balasubramanya, R. H. (2007). Biological synthesis of silver nanoparticles using the fungus *Aspergillus flavus*. *Materials Letters*, *61*, 1413–1418.

Vigneshwaran, N., Nachane, R. P., Balasubramanya, R. H., & Varadarajan, P. V. (2006). A novel one-pot 'green' synthesis of stable silver nanoparticles using soluble starch. *Carbohydrate Research*, *341*, 2012–2018.

Vinod, V. T. P., & Sashidhar, R. B. (2009). Solution and conformational properties of gum kondagogu (*Cochlospermum gossypium*)—A natural product with immense potential as a food additive. *Food Chemistry*, *116*, 686–692.

Vinod, V. T. P., Sashidhar, R. B., Sarma, V. U. M., & Saradhi, U. V. R. V. (2008). Compositional analysis and rheological properties of gum kondagogu (*Cochlospermum gossypium*): A tree gum from India. *Journal of Agricultural and Food Chemistry*, *56*, 2199–2207.

Vinod, V. T. P., Sashidhar, R. B., Sreedhar, B., Rao, B. R., Rao, T. N., & Abraham, J. T. (2009). Interaction of Pb^{2+} and Cd^{2+} with gum kondagogu (*Cochlospermum gossypium*): A natural carbohydrate polymer with biosorbent properties. *Carbohydrate Polymers*, *78*, 894–901.

Vinod, V. T. P., Sashidhar, R. B., & Sukumar, A. A. (2009). Competitive adsorption of toxic heavy metal contaminants by gum kondagogu (*Cochlospermum gossypium*): A natural hydrocolloid. *Colloids and Surfaces B: Biointerfaces*, *75*, 490–495.

Vinod, V. T. P., Sashidhar, R. B., Suresh, K. I., Rao, B. R., Saradhi, U. V. R. V., & Rao, T. P. (2008). Morphological, physico-chemical and structural characterization of gum kondagogu (*Cochlospermum gossypium*): A tree gum from India. *Food Hydrocolloids*, *22*, 899–915.

Wei, D., & Qian, W. (2008). Facile synthesis of Ag and Au nanoparticles utilizing chitosan as a mediator agent. *Colloids and Surfaces B: Biointerfaces*, *62*, 136–142.

Xiong, Y., Washio, I., Chen, J., Cai, H., Li, Z., & Xia, Y. (2006). Poly(vinyl pyrrolidone): A dual functional reductant and stabilizer for the facile synthesis of noble metal nanoplates in aqueous solutions. *Langmuir*, *22*, 8563–8570.

Xu, K., Wang, J., Kang, X., & Chen, J. (2009). Fabrication of antibacterial monodispersed Ag–SiO_2 core–shell nanoparticles with high concentration. *Materials Letters*, *63*, 31–33.

Xu, X., Yang, Q., Wang, Y., Yu, H., Chen, X., & Jing, X. (2006). Biodegradable electrospun poly(L-lactide) fibers containing antibacterial silver nanoparticles. *European Polymer Journal*, *42*, 2081–2087.

Yang, F., Wu, K.-H., Liu, M., Lin, W., & Hu, M. (2009). Evaluation of the antibacterial efficacy of bamboo charcoal/silver biological protective material. *Materials Chemistry and Physics*, *113*, 474–479.